IRIS RECOGNITION PERFORMANCE ANALYSIS

A THESIS SUBMITTED TO
THE FACULTY OF ARCHITECTURE AND ENGINEERING
OF
EPOKA UNIVERSITY

BY

ALESSIA TOLI

IN PARTIAL FULFILLMENT OF THE REQUIREMENTS
FOR
THE DEGREE OF MASTER OF SCIENCE
IN
COMPUTER ENGINEERING

JULY, 2023

Approval sheet of the Thesis

This is to certify that we have read this thesis entitled **"Iris Recognition Performance Analysis"** and that in our opinion it is fully adequate, in scope and quality, as a thesis for the degree of Master of Science.

_____

Dr. Arban Uka
Head of Department
Date: July, 13, 2023

Examining Committee Members:

Prof.Dr. Betim Çiço (Computer Engineering) _____

Dr. Arban Uka (Computer Engineering) _____

Dr. Florenc Skuka (Computer Engineering) _____

I hereby declare that all information in this document has been obtained and presented in accordance with academic rules and ethical conduct. I also declare that, as required by these rules and conduct, I have fully cited and referenced all material and results that are not original to this work.

Name Surname: Alessia Toli

Signature: _____

ABSTRACT

IRIS RECOGNITION PERFORMANCE ANALYSIS

Toli, Alessia

M.Sc., Department of Computer Engineering

Supervisor: Dr. Arban Uka

Iris recognition is among the most precise and reliable biometric authentication technologies. Technology nowadays has come to a point where it allows us to achieve iris recognition through several approaches. It is challenging, if not impossible, to compromise the authentication process as it is a reliable identifying system. Iris recognition is often applied to high-security places. In airports, port areas, access management in institutions and companies, computer login, criminal identification, mobile devices, etc are some of its areas of use. The vast majority of systems for iris recognition implement Daugman's patented algorithms, which are capable of producing successful recognition results. Yet reported results are typically obtained under suitable environments. The unique characteristics of the human iris are acquired through images in specific environments and later the images are processed in stages which include segmentation, normalization, encoding and matching. All the stages and different methods will be included in this research. All of the data in this study was obtained by using the IIT Delhi Iris Database.

Keywords: Iris Recognition, EER, Segmentation, Accuracy, FAR, FRR, Noise

ABSTRAKT

ANALIZA E PERFORMANCËS SË NJOHJES SË IRISIT

Toli, Alessia

Master Shkencor, Departamenti i Inxhinierisë Kompjuterike

Udhëheqësi: Dr. Arban Uka

Një nga teknologjitë biometrike të autentikimit më e saktë dhe më e besueshme është njohja e irisit. Sot teknologjia ndodhet në një fazë që na lejon të arrijmë njohjen e irisit nëpërmjet qasjeve të ndryshme. Është sfiduese, pothuajse e pamundur, të kompromentosh procesin e autentikimit duke qenë se është një sistem identifikues i sigurt. Njohja e irisit shpesh aplikohet në vende me siguri te lartë. Në aeroporte, zona portuale, menaxhimi i aksesit në institucione dhe kompani, hyrja në kompjuter, identifikimi kriminal, paisje elektronike etj janë disa nga fushat e përdorimit të sistemit. Shumica e sistemeve të njohjes së irisit implementojnë algoritmat e licensuara të Daugman, të cilat mundësojnë rezultate të suksesshme të njohjes. Sidoqoftë rezultatet e raportuara zakonisht janë përftuar nën mjedise të përshtatshme. Karakteristikat unike të irisit të njeriut janë fituar nëpërmjet imazheve në mjedise specifike dhe më pas imazhet janë procesuar në faza të cilat përfshijnë segmentim, normalizim, enkodim, përputhje. Të gjitha fazat dhe metodat e ndryshme do të përfshihen në këtë kërkim. Të gjitha të dhënat në këtë studim janë përftuar duke përdorur bazën e të dhënave IIT Delhi.

Fjalët kyçe: *Njohja e irisit, Segmentim, Saktesi, FAR, FRR, EER, Zhurmë*

Dedicated to my family and friends!

ACKNOWLEDGEMENTS

My sincere appreciation goes to my supervisor, Dr. Arban Uka, who provided ongoing guidance, interest, and assistance during my thesis journey. I truly value the dedication and attention he contributed to improving my academic skills during my time as a graduate.

TABLE OF CONTENTS

LIST OF TABLES

LIST OF FIGURES

LIST OF ABBREVIATIONS

FAR	False Acceptance Rate
FRR	False Rejection Rate
EER	Equal Error Rate
DoF	Degree of Freedom
Acc	Accuracy
Std	Standard Deviation
N	Number of persons
n	Number of images per person

CHAPTER 1

INTRODUCTION

1.1 Authentication and Biometrics

In iris recognition, authentication refers to the process of checking an individual's identity by comparing their extracted iris pattern to a previously enrolled template. The system checks the amount of similarity that exists between the captured iris and the registered template by evaluating the collected features and utilizing developed algorithms, which permits an appropriate decision about whether to allow or prohibit access. Authentication is essential in the field of computer science because it plays a crucial part in security. The iris does not change throughout a person's life; thus, it is very reliable for long-term authentication. It is very hard to replicate the unique patterns of the iris. That is the reason why iris recognition provides high security levels.

Biometrics is the automatic identification of persons based on distinctive physical traits, generally for safety reasons. Iris Recognition acts as a biometric system for identifying individuals based on the specific structures found in the eye's pupil. Biometric authentication systems work by obtaining some form of the feature, which might be a digital image for iris recognition. After that, the instance is converted to a biometric template via certain types of mathematical techniques. The biometric template provides a normalized version of this feature, that may then be accurately examined to various other templates to confirm the identity. The majority of biometric systems have two different ways of operating. The enrolment method, which works by adding templates into a database and also a recognition method through which a template is prepared for a person. After that an appropriate match in the database is found.

1.2 Human Iris

The human eye is a particular sensory organ that receives visual signals and transmits them via the optic nerve to the brain. It is an intricate optical structure made up of multiple interlinked elements. The iris is a prominent and colorful component in the center part of the eye that gives individuals their own distinctive eye color. The iris functions by regulating how much light reaches the eye via its main aperture, known as the pupil. It is made up of a fragile system of muscles and cells with pigment that forms structures unique to every person. These structures, which include crypts, furrows, and radial lines, stay unchanged all over time and act as a solid identifier. Iris recognition systems may correctly and safely verify persons by collecting and evaluating the exact structure and properties of these patterns, offering a very precise method for identification.

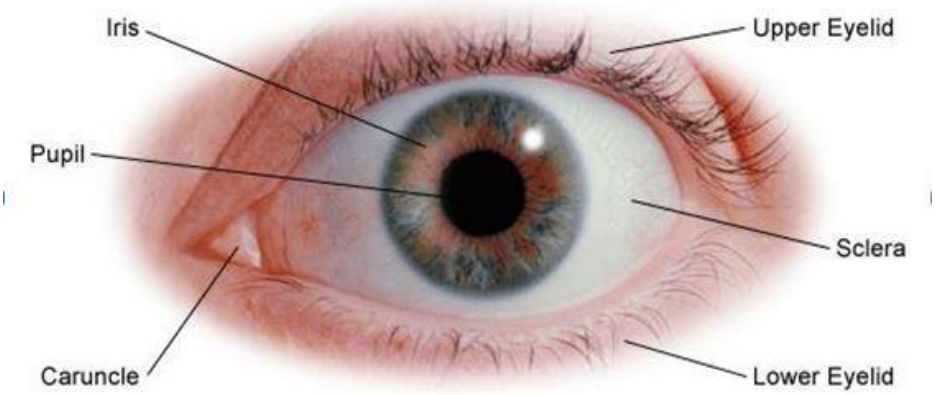

Figure 1.Human eye structure

https://drruchikaeyeclinic.com/working-of-the-eye-explained-step-by-step/

1.3 Iris Recognition

The iris develops during a person's growth phase and stays constant during the course of their lives. It is not possible to be modified clinically without risking blindness. The iris recognition systems collect, pre-process, and then evaluate high-quality pictures of the iris using advanced image processing algorithms, generally by means of near-infrared light to reveal the complex features of the iris structure. The first phase in iris recognition is to identify the iris. Through the use of

image processing techniques, we can obtain the transformed image of the eye. Next, by applying the circular Hough transform algorithm and the parabolic Hough transform algorithm, the iris, pupil, and eyelids can be identified (Efford, 2000). When the region required for analysis has been determined, the captured image must be processed onto a biometric template that consists of a mathematical model of the information stored in the iris. If an individual needs to be identified by an iris recognition system, firstly an image of the iris is taken, and then the template is stored in a database. The processed template will be compared to existing templates in the database. If it matches then the person has been recognized and if not, then the person has not been recognized and the template will be stored as a new identity.

1.4 Literature Review

The field of iris recognition has proven to be a particularly robust and reliable biometric system, having benefits like stability over time and unique characteristics among individuals. This review covers the latest breakthroughs, difficulties, and findings in the field of iris recognition, referring to the studies of different authors.

Daugman's research (2007, 2009) laid the foundation for modern iris recognition by introducing innovative techniques in iris encoding and matching and offering a comprehensive understanding of the complex process of iris recognition. Furthermore, the study conducted by Ng, Tay, & Mok (2008) provides an analytical comparison of different iris recognition algorithms, giving an understanding of their efficacy and execution.

Segmentation, the method of isolating the iris from other eye structures, is a vital component of iris recognition. Uka, Roçi, & Koç (2017) presented an enhanced segmentation algorithm, revealing promising results in terms of efficiency and accuracy. This is essential in addressing complex iris recognition situations, setting the basis for subsequent processing stages.

The evolution of encoding techniques has largely contributed to the progression of iris recognition. Oktay, Albana, & Arban suggested another approach to iris encoding, offering a new angle on the conversion of iris patterns into

mathematical constructs. Also, Koç & Uka (2016) developed a new encoding method using eight quantization levels, illustrating an effective method of capturing fine iris details.

Additionally, Koç & Uka's study explored the application of the 1D Fourier Transform for iris recognition. Their research shows promise in dealing with changes in lighnting and orientation, confirming the effectiveness of frequency domain-based techniques in iris recognition.

The performance of iris recognition systems has been the focus of ongoing research. A study by Koç, Roçi, & Uka (2019) evaluated the performance of iris recognition by using classical and trapezoidal-shaped templates combined with an advanced iris segmentation technique. Their research provides essential understanding of the impact of template shape on recognition precision.

Furthermore, Koç et al. (2020) evaluated the performance of iris recognition under non-cooperative conditions, making a significant contribution to the development of practical, real-world iris recognition systems.

The capabilities of advanced methods, such as convolutional neural networks (CNNs), to improve iris recognition performance has been a recent study. For example, Koc, Balla, & Uka (2019) assessed the performance of CNNs in iris biometrics, focusing especially on noisy iris images. Their research suggests that advanced machine learning methods could be crucial in dealing with complex challenges, such as noise, in iris recognition.

Despite considerable advancements, several issues, such as noise management and improving recognition under non-cooperative circumstances, still exist. Iris recognition has experienced significant progress over time, driven by constant research in segmentation, encoding, and optimization techniques. The integration of advanced strategies, like machine learning, facilitates future research.

The practical applications of iris recognition technology have increased over the years due to technological and theoretical progress.

One noticeable application is the application of iris recognition in healthcare systems (Koç et al., 2020). Iris recognition offers a reliable method of identification, used for managing patient identities, providing access to individual medical records,

and enhancing the efficiency of healthcare delivery. It excludes the risk of identity confusion, improving the safety and security of medical practices.

Another growing application area is mobile technology. As smartphones become essential parts of our daily lives, securing the data within these devices is of maximum importance. Iris recognition provides a user-friendly and highly secure way of locking and unlocking devices, adding an extra security layer to traditional methods like passcodes or fingerprint recognition.

Despite the impressive advancements in iris recognition research and application, a few challenges continue to hide its full potential. These mainly include issues related to image quality, occlusions, and changes in lighting conditions.

The problem of image quality, particularly in non-cooperative scenarios or with noisy iris images, is a significant problem. Muda (2019) and Koc, Balla, & Uka (2019) dive into this issue, studying how noise can lower the performance of iris recognition systems and suggesting potential methods to improve these effects. Their studies contribute in strengthening the robustness of iris recognition in practical cases.

Another challenge is dealing with occlusions caused by eyelids and eyelashes. Ongoing research is centered at developing robust segmentation algorithms that can accurately distinguish the iris from these and other eye features, and Uka, Roçi, & Koç's work (2017) is a considerable contribution in this field.

The evolution of iris recognition, from its theoretical origins to modern implementations, is proof to the continuing technological growth and transformation in this area. The challenges, such as managing noise and occlusions, show chances for more exploration and development. As research proceeds, it is expected that the reliability and robustness of iris recognition will further improve, establishing its position as a leading biometric technology.

1.5 Thesis purpose

This thesis starts with general information about biometrics and its applications in everyday life. Then it continues with a brief explanation of how iris recognition systems work. Next, the iris and its structure are explained in generic

terms. Furthermore, some information regarding the iris recognition technology, algorithms, and techniques used in the system is presented. This thesis will cover the fundamental concepts regarding the stages of iris recognition such as segmentation, normalization, encoding, matching, and so on. Based on already published articles about iris recognition and codes generated in the MATLAB software, many tests have been made. Different segmentations and encodings will be compared. As an input, the IIT-Delhi iris dataset has been used.

1.6 IIT Delhi Iris Database

The database used in this thesis is the IIT Delhi (Indian Institute of Technology) Iris Database version 1.0. The database consists of 2240 images. There are 224 people and each one of them has 10 images, 5 for the left eye and 5 for the right eye. The images are taken using JIRIS, JPC1000 and digital CMOS camera in an indoor area. Each image is 320 x 240 pixels in size and is saved in bitmap format. The iris database folder is organised in 224 subfolders with 10 images each.

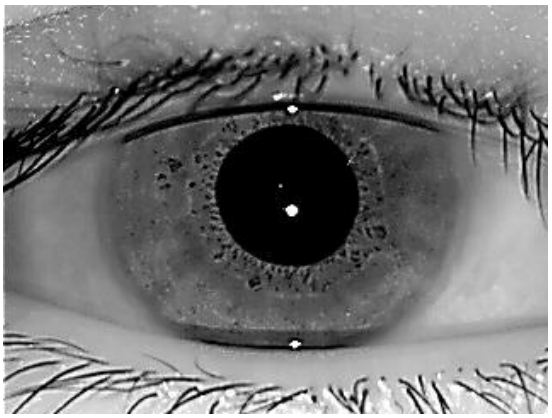

Figure 2.Example of iris image from IIT database (person 15, pic no.1)

CHAPTER 2

IRIS RECOGNITION STEPS

2.1 Segmentation

Iris segmentation [1] is the automatic recognition of the iris and pupil boundaries of an iris in an image with the intention of eliminating the regions that surround it. This procedure allows to correctly and clearly retrieve characteristics from the iris for identification purposes.

In simpler terms, the main goal of segmentation is to remove unnecessary regions that include those beyond the iris (skin, eyelids, eyelashes) [2]. The level of quality of the image determines the success of the segmentation. Different approaches, like the integro-differential operators, such as Daugman's or Hough Transform, can be used to isolate the iris [3][4][5]. The step of segmentation defines the iris and pupil boundaries, which later get converted to an appropriate template during the normalization step.

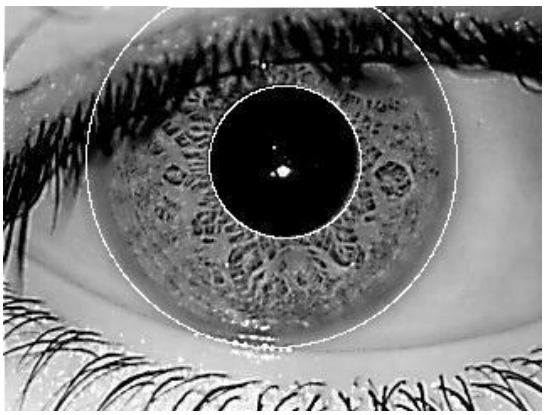

Figure 3.Example of iris image segmented (person 100, pic no.2)

2.1.1. Hough Transform

The Hough Transform is an important and commonly used approach in iris recognition for the essential task of detecting the iris and pupil boundary, which is part of the segmentation process. It is a method for extracting features that detects simple patterns in an image like circles, lines, and ellipses. It begins by producing an edge map that is based on the first derivatives of the pixel values and then thresholding the resultant image. In such a way, it determines both of the circles where the iris is placed in-between. The derivatives that lie in the horizontal direction detect the eyelids, while the derivatives that lie in the vertical direction detect the iris (Efford, 2000) (Pan & Xie, 2005).

2.1.2. Noise Detection

Detecting eyelashes may interfere with iris recognition, that's why Kong and Zhang developed an appropriate technique. Their technique categorizes eyelashes into two main groups: separable eyelashes and multiple eyelashes. The separation is essential because it impacts the technique used.

To detect the first group correctly, Kong and Zhang made use of 1D Gabor filters. The basic idea is that when a separable eyelash is convoluted with the Gaussian smoothing function, the output value is simply low. The detection of eyelashes that belong to the second group, known as multiple eyelashes, requires a different approach. Multiple eyelashes can be distinguished by their dense nature, which makes individual detection difficult. To address this, Kong and Zhang recommended using intensity variance. Their approach involves scanning a small window across the image and computing the intensity variance within that area. If the variance is less than a certain threshold, it is assumed that the center of the window corresponds to a point on an eyelash. This technique takes advantage of the fact that eyelashes have a uniform intensity that differs from other eye features.

2.1.3. Adding Noise

The variety of persons, the kind of camera and wavelength utilized for image collection, the brightness of the background, and the shadows created by eyelids and eyelashes can all have a direct effect on the efficacy of iris recognition. Given these considerations, the overall quality of images in the dataset was intentionally dropped by adding noise. two sorts of noise could be used, in particular: Gaussian noise and Salt-and-pepper noise.

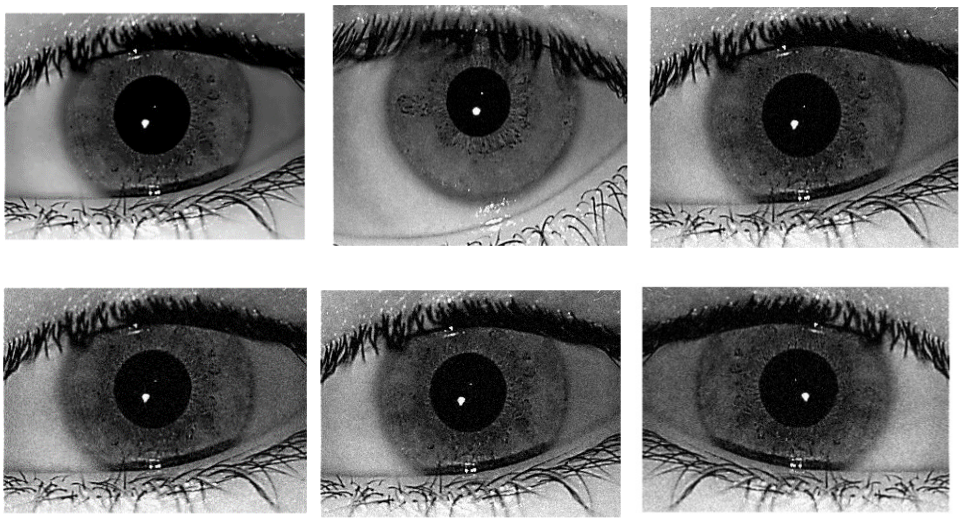

Figure 4.Example of iris image with 0 noise, 0.001 noise, 0.002 noise, 0.003 noise, 0.004 noise, 0.005 noise.

2.2 Normalization

After the first phase, we get a segmented image. The second phase in the recognition process is to normalize the iris region. During normalization, the aim is to obtain an extracted iris template that you can compare to other irises. The primary objective of this stage is to correct dimensional discrepancies caused by a variety of factors such as iris stretching due to pupil enlargement when light intensity changes, the distance, changed head position, and movement of the eye inside the cavity of the eye. Daugman's Rubber Sheet Model normalizes irises and creates templates that can be compared to one another. The model is meant to convert the two-dimensional structure of the iris to a simple rectangular format. Daugman's Rubber Sheet Model operates by translating every point within the iris into a set of polar coordinates - with a radius 'r' and an angle 'theta'.

(b)Figure 5. (a) iris region; (b) iris region mask after the process of normalization

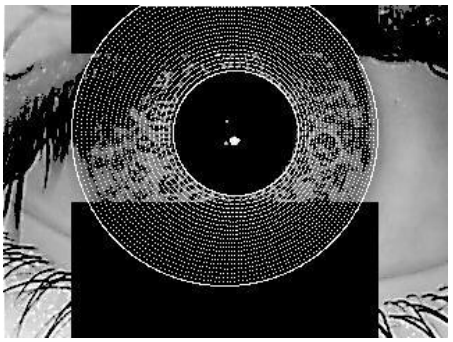

Figure 6.Person 100, Image 2 after Normalization process

2.3 Encoding

Encoding is the process of converting a person's individual iris patterns into a digital representation that can then be properly archived and compared. Following image acquisition and preprocessing, the unique shapes of the iris are transformed into a biometric template via an encoding technique. The use of Gabor filters or Daugman's 2D Gabor wavelets to acquire features of the iris is a typical encoding approach.

This thesis employs three distinct encoding techniques. The first, E1, is known to be the conventional one because it is the version that Daugman implements in his approach. The phase space is split into four quadrants, each of which is fifty percent different from the others. As illustrated in the image below, each of the quadrants is [11], [01], [00], and [10]. Since every pixel can be represented with two bits, this encoding produces a 20x480 matrix template of data on the phase.

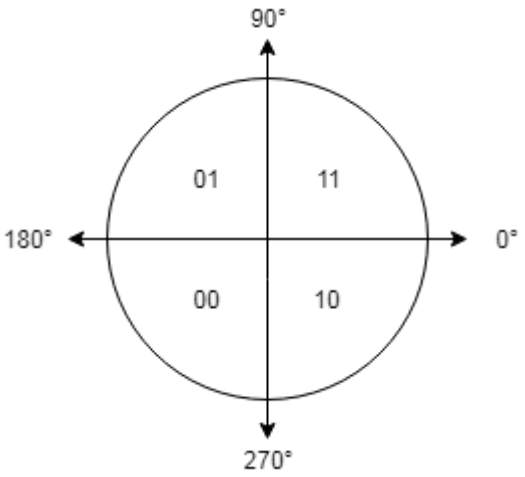

Figure 7.E1

As represented in the picture below, the second encoding method E2, transforms the phase space into four quadrants, where every one is 33% different compared to the neighboring quadrants. The generated template will consist of a 20x720 matrix.

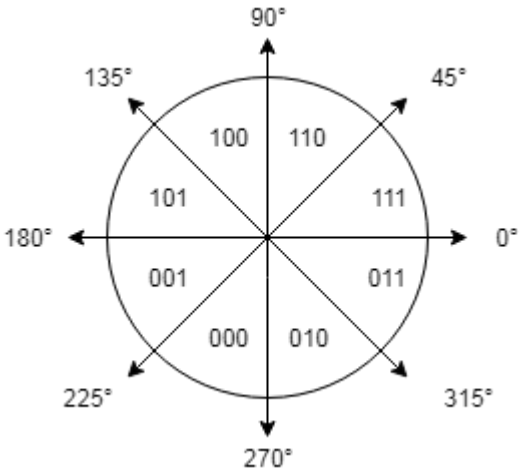

Figure 8. E2

The third encoding, E3, quantizes the space into four quadrants, each of which is 25% different compared to other neighboring quadrants and 100% different from opposing quadrants, as seen below. The generated template is a 20x960 matrix.

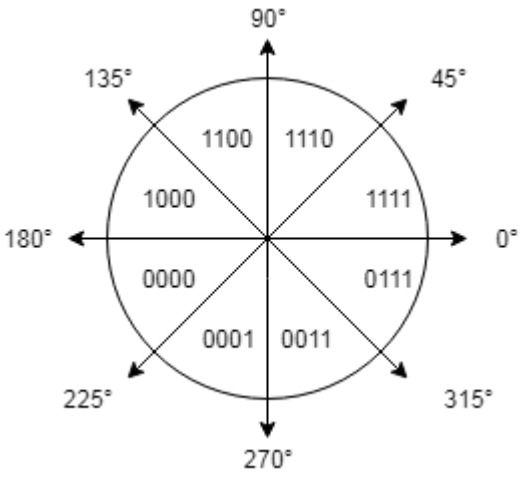

Figure 9.E3

2.4 Matching

The template developed during the feature encoding step requires a matching metric, that provides an evaluation of similarity among two iris templates. You can compare the different or the same iris. The terms for these comparisons are inter-class and intra-class respectively. Because of the masked information, Hamming Distance was chosen to be the matching metric. Each of these cases is expected to generate separate and individual values, allowing a choice to be reached when determining if the two templates originate from the same iris or two different irises. To produce a satisfactory matching process while accounting for noise or head turns, the templates go through an 8-bit shifting operation in both the left and right directions when computing the hamming distance.

i)

CHAPTER 3

METHODOLOGY

In this study, combinations of different segmentations and encodings were tested using the IIT Delhi Iris Database. These tests were made using a rectangular template. The segmentations used are Masek's algorithm (S1), a segmentation suggested by Liu, Bowyer, Flynn (S2) and EPK_IRIS (S3). The encodings are referred to as E1, E2 and E3. The experimental results were made by making a combination of the segmentations and encodings mentioned previously, which resulted in S1E1, S1E2, S1E3, S2E3, S3E1, S3E2, S3E3. Firstly 5 sets of 20 random people were selected. Each person in the dataset has 5 images of the left eye and 5 images of the right eye. The first 13 persons in the dataset do not have images of both their eyes, they only have 10 images of their left eye and that is the reason why they have not been used in the experiments. After having the sets, new images are created by applying variance values of Gaussian noise. Each set will have an initial noise of 0, then the sets will have variance values of 0.001, 0.002, 0.003, 0.004 and 0.005. After running all the sets with different segmentation techniques and applying to each set different Gaussian noise, the results were recorded in order to be analyzed.

Below are several iris images demonstrating the improvement of segmentation for a noise value of 0.004 over the set of 20 individuals, showing a considerable reduction of the EER.

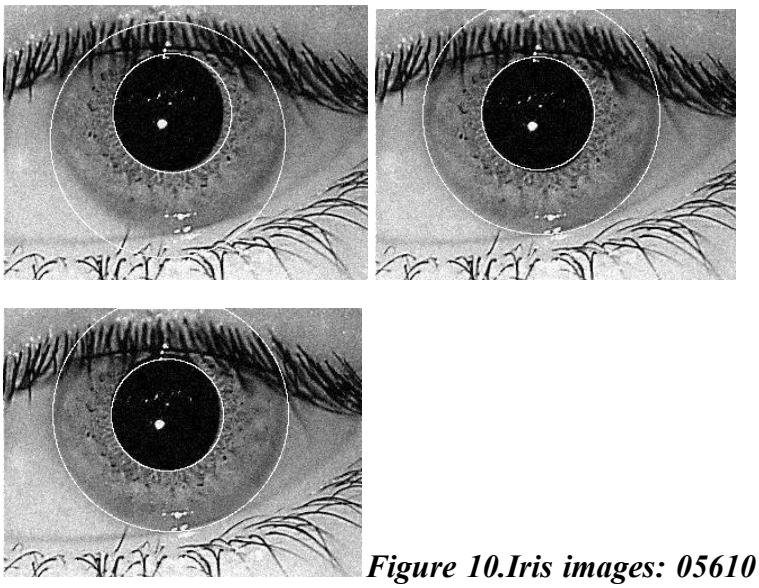

Figure 10.Iris images: 05610 IIT Delhi after S1 (first), S2 (second) and, S3 (third)

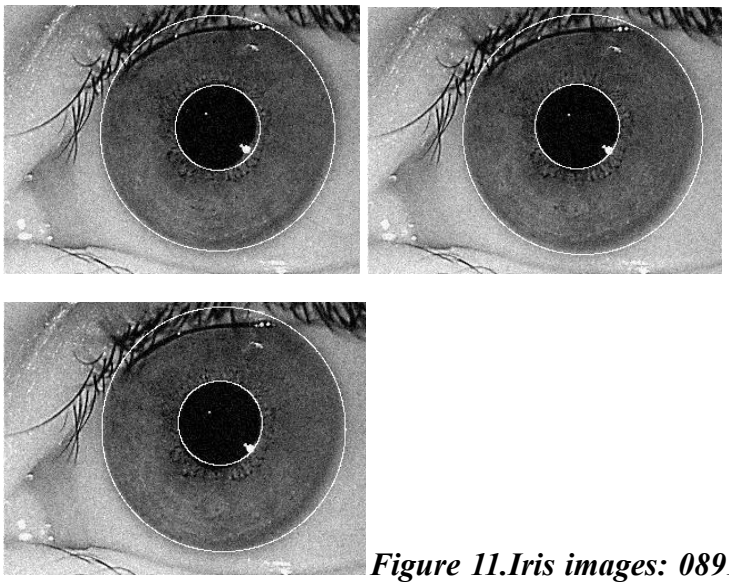

Figure 11.Iris images: 08910 IIT Delhi after S1 (first), S2 (second) and, S3 (third)

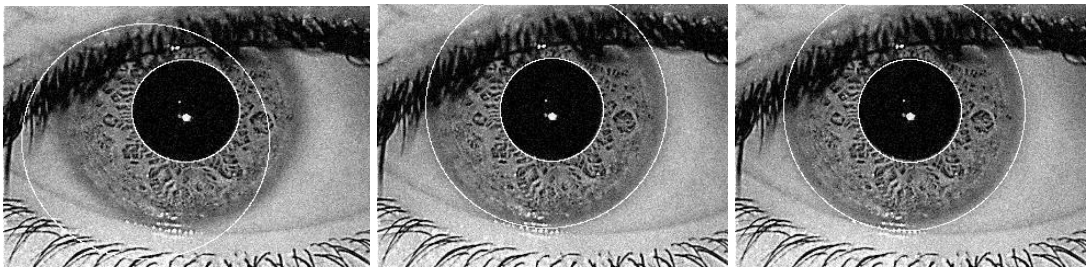

Figure 12.Iris images: 10005 IIT Delhi after S1 (first), S2 (second) and, S3 (third)

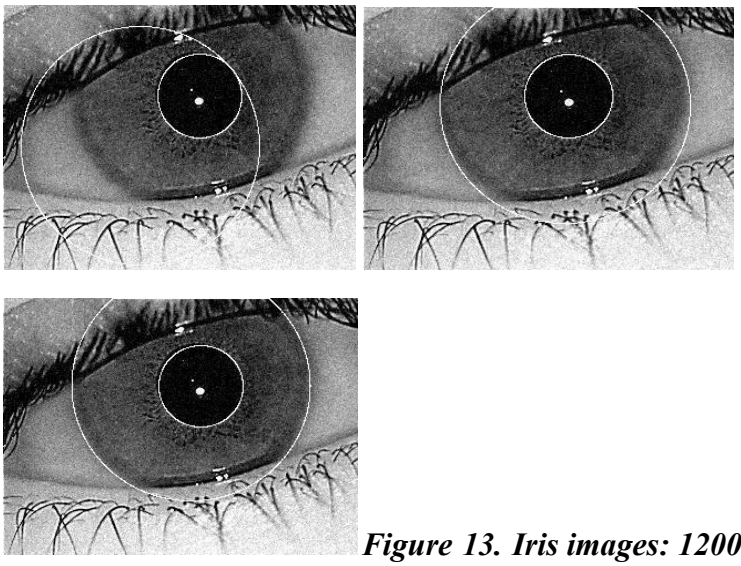

Figure 13. Iris images: 12004 IIT Delhi after S1 (first), S2 (second) and, S3 (third)

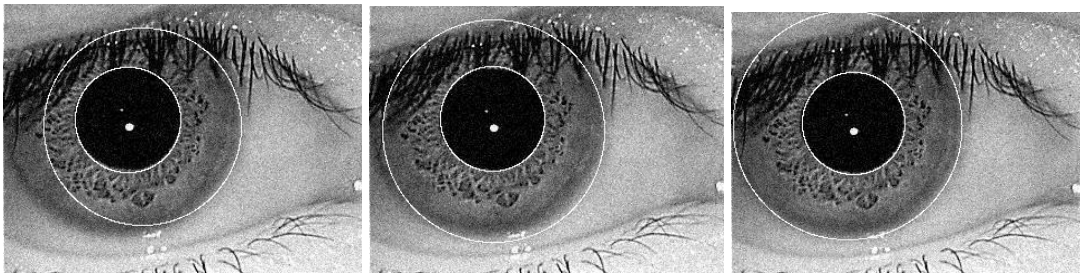

Figure 14.Iris images: 20102 IIT Delhi after S1 (first), S2 (second) and, S3 (third)

During the experiments, the most important calculations included the following: FAR, FRR, EER, INTER, INTRA, accuracy, DoF and dprime.

FAR stands for False Acceptance Rate. If the iris recognition system detects an iris pattern that isn't associated with the specified user but provides access regardless, this is considered a false acceptance. The FAR is frequently represented as a percentage, a smaller percentage indicating a better precision system.

FAR is calculated as follows:

$$FAR(n) = \frac{Number\ of\ successful\ imposter\ attempts\ for\ a\ qualified\ individual\ n}{Total\ number\ of\ imposter\ attempts\ for\ that\ qualified\ individual\ n}$$

$$FAR = \frac{1}{N}\sum_{n=1}^{N} FAR(n)$$

Equation 7. *FAR*

FRR stands for False Rejection Rate. A false rejection occurs when an actual authorized person attempts to be recognized by the iris recognition system but the system wrongly denies access. The FRR, similar to the FAR, is expressed as a percentage, so a lower percentage suggests a more precise system.

FRR is calculated as follows:

$$FRR(n) = \frac{Number\ of\ rejected\ verification\ attempts\ for\ a\ qualified\ individual\ n}{Total\ number\ of\ verification\ attempts\ for\ that\ qualified\ individual\ n}$$

$$FRR = \frac{1}{N}\sum_{n=1}^{N} FRR(n)$$

Equation 8. *FRR*

EER stands for Equal Error Rate. The Equal Error Rate is the intersection point of False Acceptance Rate (FAR) and False Rejection Rate (FRR). In order to find EER, the values of FAR nad FRR should be plotted. Their intersection will give the EER.

An intra-class comparison is between different images of the same person's iris. For example, comparing an iris image captured today with an image captured a week ago for the same person would be an intra-class comparison.

An inter-class comparison is between images of different individuals' irises. For example, comparing the iris image of person A with that of person B would be an inter-class comparison.

They are calculated as follows:

$$N_{intra} = N \cdot \frac{n!}{(n-2)! \cdot 2!}$$ ***Equation 1.***

$$N_{inter} = n^2 \bullet \frac{(N-1) \cdot N}{2}$$ ***Equation 2.***

The next calculation is Accuracy. Accuracy is a measure of how well the system correctly identifies or verifies individuals.

Accuracy is calculated as follows:

$$Accuracy = \frac{TP \cdot intra + TN \cdot inter}{inter + intra} \cdot 100\%$$

Equation 9. *Accuracy*

True Positive (TP), True Negative (TN), False Positive (FP), and False Negative (FN) are used to measure the performance of the iris system. The following are the definitions for these terms:

1. True Positive (TP): An instance where the system correctly identifies or verifies an authorized user.
2. True Negative (TN): An instance where the system correctly identifies an unauthorized user and rejects their access.
3. False Positive (FP): An instance where the system incorrectly identifies or verifies an unauthorized user (related to FAR).
4. False Negative (FN): An instance where the system incorrectly fails to identify or verify an authorized user (related to FRR).

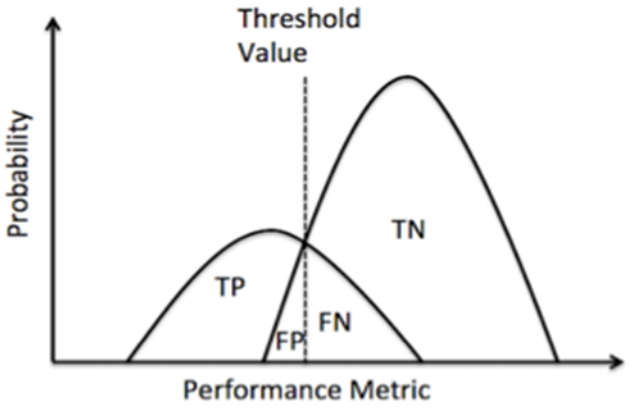

Figure 15.Performance metric parameter *[15]*

The term "degree of freedom" refers to the variety or uniqueness that comes from iris patterns. We are able to compute it using the mean and standard deviation of the interclass values.

DoF is calculated as follows:

$$DOF = \frac{\mu_{inter}(1-\mu_{inter})}{\sigma^2_{inter}}$$

Equation 4. *Degrees of Freedom*

Decidability, known as d', is a measure of how distinct intra-class comparisons are against inter-class comparisons. The higher the value of d', the more successful the system is in separating inter-class and intra-class distributions.

Dprime is calculated as follows:

$$d\ prime = \frac{|\mu_{intra}-\mu_{inter}|}{\sqrt{\frac{\sigma^2_{intra}+\sigma^2_{inter}}{2}}}$$

Equation 5. Decidability, D Prime

CHAPTER 4

RESULTS AND DISCUSSIONS

To compare the accuracy and Equal Error Rate (EER) of different segmentation and encoding methods, analysis was conducted using random datasets taken from the IIT Delhi database. Specifically, the S1, S2 and S3 segmentation methods were examined, along with the E1, E2 and E3 encoding methods. Some other comparisons were made regarding the Degree of Freedom and dprime of each set. For every combination of segmentation and encoding, which consisted of 20 random persons, an addition was made to the experiments, which consisted in changing the number of images per person. The iris photos utilized in these tests were selected randomly, without any regard to their quality or suitability.

The findings from S1 E1, S1 E2, S1 E3, S2 E3, S3 E1, S3 E2 and S3 E3 can also be visually represented. The provided tables present data related to the performance of the iris system under various conditions. The next tables show the

average accuracy, average EER and the standard deviation of each respectively for 5 sets of 20 individuals with Gaussian noise from 0 up to 0.005.

N=20	Noise	Accuracy	Acc stdev	EER	EER stdev
S1 E1	0	98.4733245	0.146727378	20.49400425	2.234926844
	0.001	98.39641766	0.042928108	23.7812828	1.163876849
	0.002	98.40479384	0.043543476	25.88178923	2.042867032
	0.003	98.40144143	0.043264731	26.72094352	0.454704505
	0.004	98.40341883	0.046391015	27.58653592	1.521122628
	0.005	98.40569678	0.039625215	27.50126158	1.417389082
	Mean	98.41418217		25.32763621	
	Stdev	0.029160629		2.750668019	

Table 1.Accuracy and EER for N=20, S1 E1

N=20	Noise	Accuracy	Acc stdev	EER	EER stdev
S1 E2	0	99.758504	0.1367247	8.6866717	4.4687005
	0.001	99.736802	0.1561974	8.3446065	3.7271965
	0.002	99.678088	0.1952347	9.6988145	4.2120246
	0.003	99.662477	0.2349992	9.4924336	5.7358331
	0.004	99.626358	0.20829	10.601351	3.4225824
	0.005	99.590049	0.1991294	10.187962	3.2834874
	Mean	99.675379		9.5019732	
	Stdev	0.0640946		0.8628167	

Table 2.Accuracy and EER for N=20, S1 E2

N=20	Noise	Accuracy	Acc stdev	EER	EER stdev
S1 E3	0	98.4266529	0.02447248	17.0036962	17.0036962
	0.001	98.4166031	0.03948463	22.9377011	2.39391628
	0.002	98.4245502	0.04298902	26.2026086	2.91430596
	0.003	98.4188825	0.03079322	28.536958	3.44712072
	0.004	98.4095061	0.02900466	31.961386	2.9486391

	0.005	98.4144534	0.03157304	33.6959319	2.42259375
	Mean	98.418441		26.7230469	
	Stdev	0.0063884		6.13868181	

Table 3.Accuracy and EER for N=20, S1 E3

N=20	Noise	Accuracy	Acc stdev	EER	EER stdev
S2 E3	**0**	98.93795248	0.740164354	13.10751703	4.785939421
	0.001	98.92675869	0.732313042	16.75500784	6.127458364
	0.002	98.91552114	0.726417708	19.33203371	9.274968758
	0.003	98.8885677	0.679381015	22.79503411	10.84770181
	0.004	98.8689142	0.664394685	24.65662663	11.8265215
	0.005	98.85834614	0.654195126	26.68107153	12.06758228
	Mean	98.8993433916		20.55454847	
	Stdev	0.03233204511		5.1141066579	

Table 4.Accuracy and EER for N=20, S2 E3

N=20	Noise	Accuracy	Acc stdev	EER	EER stdev
S3 E1	**0**	99.98575178	0.012265038	0.523238095	0.486279596
	0.001	99.94675666	0.044238115	2.668952381	2.365732364
	0.002	99.94825647	0.028971045	2.146095238	1.405449807
	0.003	99.9167604	0.059486524	3.140190476	2.43818242
	0.004	99.87476565	0.057576978	4.007238095	2.62481215
	0.005	99.83727034	0.095026765	3.519619048	2.565391025
	Mean	99.91826021666		2.6675555555	
	Stdev	0.054259230587		1.2340312358	

Table 5.Accuracy and EER for N=20, S3 E1

N=20	Noise	Accuracy	Acc stdev	EER	EER stdev
S3 E2	0	99.98226	0.0175924	0.3357143	0.397398
	0.001	99.930906	0.0521331	2.9104762	2.4182704
	0.002	99.933707	0.0603669	2.2447619	2.3105094
	0.003	99.894491	0.0571395	2.6380952	2.0833755
	0.004	99.873016	0.0606371	3.0085714	2.1083032
	0.005	99.807656	0.0939756	3.9357143	2.9238895
	Mean	99.9036726		2.51222221	
	Stdev	0.06010494		1.20464635	

Table 6.Accuracy and EER for N=20, S3 E2

N=20	Noise	Accuracy	Acc stdev	EER	EER stdev
S3 E3	0	99.9820023	0.01509157	0.42914286	0.42586638
	0.001	99.9212598	0.06115301	3.43466667	2.66299991
	0.002	99.9183631	0.07613468	3.00466667	2.33369119
	0.003	99.8839116	0.08604704	3.75390476	2.79523433
	0.004	99.8668622	0.0704576	4.44257143	3.07389561
	0.005	99.8046347	0.08385153	3.4750702	3.4750702
	Mean	99.8961722		3.0900037	
	Stdev	0.05979488		1.38742464	

Table 7.Accuracy and EER for N=20, S3 E3

The next tables will show the results of the average DoF, average dprime and the standard deviations of each respectively for 5 sets of 20 random persons with Gaussian noise varying form 0 up to 0.005 belonging to all the different segmentations.

N=20	Noise	DoF	DoF stdev	dprime	dprime stdev
S1 E1	0	31.90	6.49429027	0.687460843	0.094231149
	0.001	33.76072133	8.416799838	0.65810833	0.101239242
	0.002	35.08723982	8.968295581	0.613966704	0.082382968
	0.003	36.22811334	9.407824464	0.541064297	0.029473693
	0.004	37.97973659	10.42864829	0.494416401	0.003727185
	0.005	39.18193939	10.63216619	0.532027622	0.046990418
	Mean	3.57E+01		0.588	
	Stdev	2.69E+00		0.0769	

Table 8.DoF and dprime EER for N=20, S1 E1

N=20	Noise	DoF	Dof stdev	dprime	Dprime stdev
S1 E2	0	2.97E+03	6.29E+02	1.878229	0.532197
	0.001	3.53E+03	6.40E+02	1.6838214	0.4231756
	0.002	3.90E+03	6.33E+02	1.6122425	0.5336824
	0.003	4.14E+03	6.88E+02	1.4919151	0.3976494
	0.004	4.33E+03	8.33E+02	1.3860648	0.3351931
	0.005	4.76E+03	6.77E+02	1.3244176	0.3431989
	Mean	3.94E+03		1.56	
	Stdev	6.29E+02		0.205	

Table 9.DoF and dprime EER for N=20, S1 E2

N=20	Noise	DoF	Dof stdev	dprime	Dprime stdev
S1 E3	0	5.14E+01	3.40E+01	0.71784298	0.12096171
	0.001	4.76E+01	2.65E+01	0.41250275	0.41250275
	0.002	4.57E+01	2.50E+01	0.49869355	0.49869355

	0.003	4.31E+01	4.31E+01	0.41247165	0.41247165
	0.004	4.33E+01	2.21E+01	NaN	NaN
	0.005	4.19E+01	2.00E+01	NaN	NaN
	Mean	4.55E+01		0.51	
	Stdev	3.54E+00		0.144	

Table 10.DoF and dprime EER for N=20, S1 E3

N=20	**Noise**	**DoF**	**DoF stdev**	**dprime**	**Dprime stdev**
S2 E3	**0**	1.26E+03	1.68E+03	1.211210751	0.501165491
	0.001	1.50E+03	2.00E+03	1.145794938	0.499322504
	0.002	1.61E+03	2.17E+03	0.897889183	0.600644165
	0.003	1.87E+03	2.49E+03	0.936090318	0.508767818
	0.004	1.84E+03	2.47E+03	0.890831161	0.507764577
	0.005	2.01E+03	2.73E+03	1.142744086	0.077266735
	Mean	1.68E+03		1.04	
	Stdev	2.77E+02		0.144	

Table 11.DoF and dprime EER for N=20, S2 E3

N=20	**Noise**	**DoF**	**DoF stdev**	**dprime**	**dprime stdev**
S3 E1	**0**	1.64E+03	2.03E+02	3.810215172	0.636701681
	0.001	1.86E+03	2.05E+02	2.883032514	0.879313995
	0.002	1.96E+03	2.43E+02	2.677741502	0.629896536
	0.003	2.01E+03	2.19E+02	2.308349775	0.643527106
	0.004	2.09E+03	2.83E+02	2.118575391	0.532085404
	0.005	2.10E+03	3.72E+02	1.961910354	0.417491571
	Mean	1.94E+03		2.63	
	Stdev	1.73E+02		0.674	

Table 12.DoF and dprime EER for N=20, S3 E1

N=20	Noise	DoF	DoF stdev	dprime	dprime stdev
S3 E2	0	3.31E+03	3.42E+02	3.5474745	0.7102178
	0.001	3.79E+03	2.87E+02	2.8912502	0.8671693
	0.002	4.07E+03	3.37E+02	2.5035758	0.7427778
	0.003	4.23E+03	3.21E+02	2.1323711	0.5382198
	0.004	4.39E+03	4.73E+02	1.8963718	0.3721631
	0.005	4.40E+03	3.55E+02	1.7982807	0.449556
	Mean	4.03E+03		2.46	
	Stdev	4.20E+02		0.668	

Table 13.DoF and dprime EER for N=20, S3 E2

N=20	Noise	DoF	DoF stdev	dprime	dprime stdev
S3 E3	0	1.72E+03	1.25E+02	3.79919764	0.70633785
	0.001	1.91E+03	1.56E+02	2.83513944	1.01696982
	0.002	2.03E+03	1.89E+02	2.56613687	0.90152172
	0.003	2.15E+03	3.25E+02	2.21219782	0.6582676
	0.004	2.28E+03	3.10E+02	1.96739851	0.46178786
	0.005	2.22E+03	3.78E+02	1.80896259	0.42648144
	Mean	2.05E+03		2.531505478	
	Stdev	2.10E+02		0.7270046231	

Table 14.DoF and dprime EER for N=20, S3 E3

As mentioned previously, four key metrics are examined - Accuracy, Equal Error Rate (EER), Degree of Freedom (DoF), and dprime. These results come from different system combinations denoted as S1 E1, S1 E2, S1 E3, S2 E3, S3 E1, S3 E2, and S3 E3.

Noise: This is the amount of unwanted disturbance in the data that can interfere with the recognition process. In this context, it is seen that as noise levels increase, it negatively affects the other metrics, causing a decrease in system performance.

Accuracy: This metric represents the percentage of correct iris recognition cases. The higher the accuracy, the more reliable the system. Across all the combinations, accuracy generally decreases as the noise increases, which is expected as higher noise levels can faint the unique iris patterns the system is trying to detect. However, the degree of impact differs across the segmentations. The combinations S3 E1, S3 E2, and S3 E3 appear the most robust, with average accuracies around 99.9% despite increased noise. On the other hand, S1 E1, S1 E3, and S2 E3 have lower average accuracies, ranging from about 98.4% to 98.9%.

Equal Error Rate (EER): The EER is the point where the rates of False Acceptance and False Rejection are equal. A lower EER is wanted as it indicates fewer overall errors. Here again, S3 E1, S3 E2, and S3 E3 perform the best with average EERs between 2.5 and 3.1, despite increased noise. This suggests that these combinations provide a good balance between avoiding errors. In contrast, S1 E1, S1 E2, S1 E3, and S2 E3 combinations have higher average EERs, indicating less optimal performance.

Degree of Freedom (DoF): DoF represents the uniqueness in the system. In these results, the highest DoF values occur in configurations S1 E2, S3 E2, and S3 E3, implying these systems might have the most complex setups.

dprime: This is a measure of statistical effect size - evaluates the separation of inter class distribution and intra class distribution. A higher dprime value indicates a bigger separation, meaning a more correct recognition. Generally, as noise increases, the dprime value decreases, reflecting that the system's ability to distinguish between different irises deteriorates with the introduction of more noise. This trend is observed across all combinations.

Acc stdev (Standard Deviation of Accuracy): This measures the amount of variation or dispersion from the average accuracy. A low standard deviation indicates that the accuracy values tend to be close to the mean (average) accuracy value, while

a high standard deviation indicates that the accuracy values are spread out over a wider range.

EER stdev (Standard Deviation of EER): Similar to Acc stdev, this measures the variation or dispersion from the average EER. A low standard deviation indicates that the EERs are close to the mean EER, while a high standard deviation indicates they are spread out over a wider range.

DoF stdev: This value represents the standard deviation of the Degree of Freedom. A smaller standard deviation indicates that the DoF values are closely clustered around the mean (average) DoF value, meaning the system's DoF is relatively consistent under different conditions. A larger standard deviation indicates that the DoF values are spread out over a larger range, suggesting the system's DoF varies more significantly under different conditions.

dprime stdev: This value represents the standard deviation of the d-prime values. Similarly, a smaller standard deviation here suggests that the system's d-prime is consistent under different conditions, while a larger standard deviation indicates more variability in the d-prime.

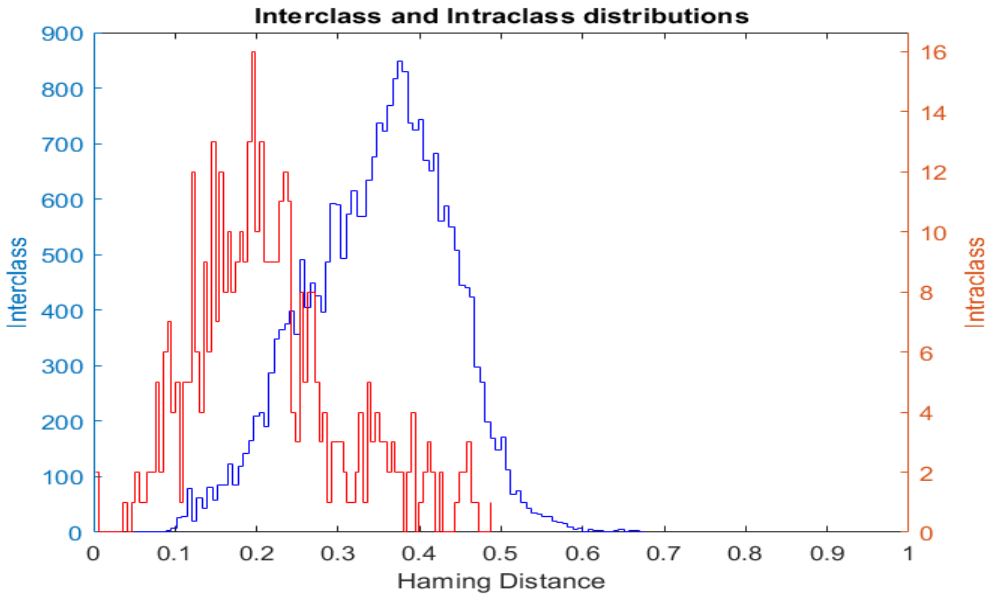

Figure 16. Histogram for S1 segmentation N=20, n=10

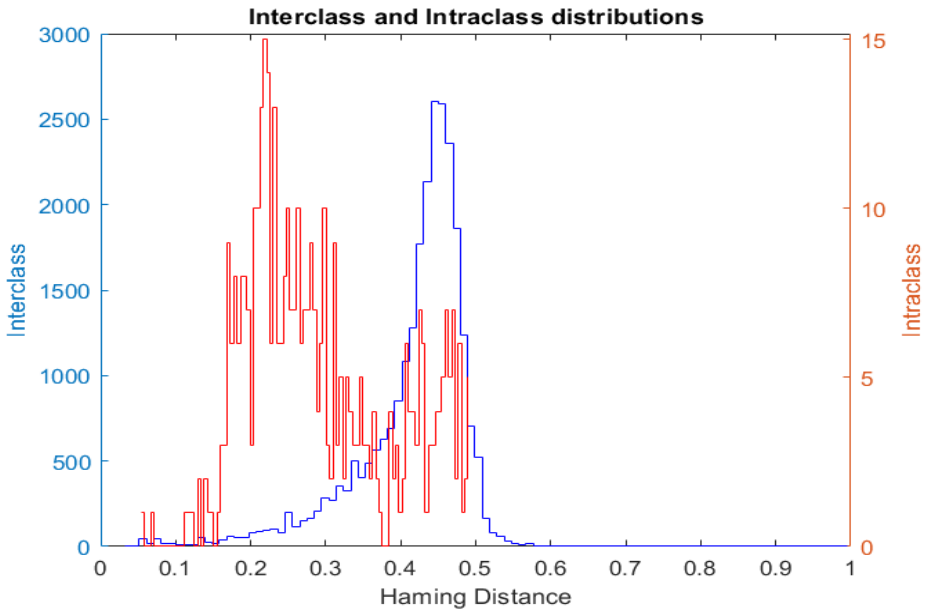

Figure 17. Histogram for S2 segmentation N=20, n=10

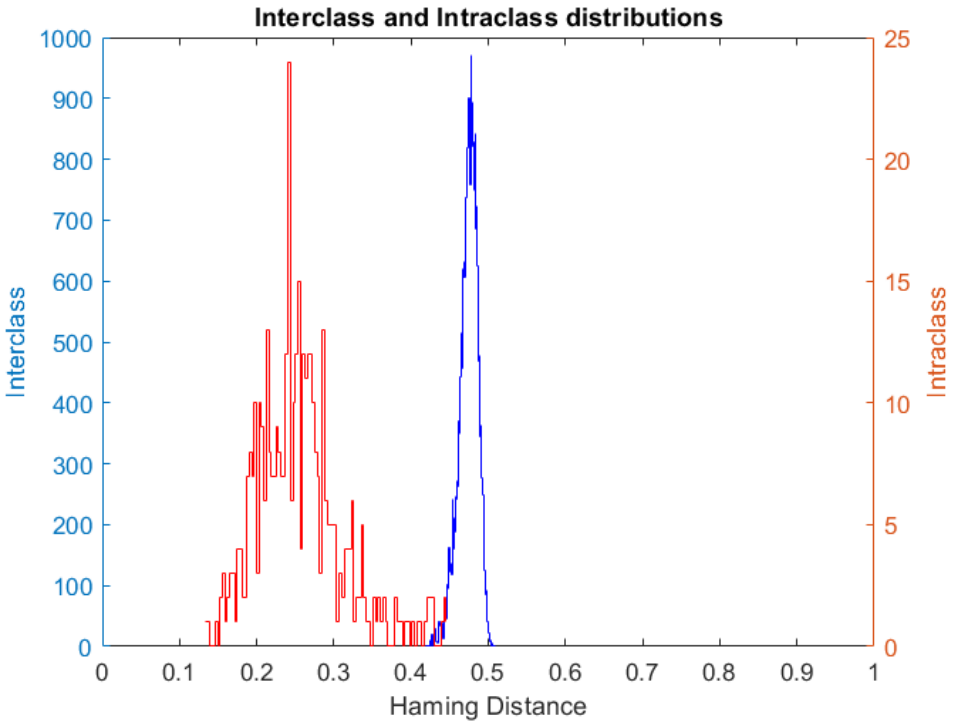

Figure 18. Histogram for S3 segmentation N=20, n=10

Figures 16, 17 and 18 illustrates three different histograms for 20 individuals from the IIT Delhi iris database using 3 segmentations, S1, S2 and S3. Figure 16 represents the resulting histogram from S1. Figure 17 represents the

resulting histogram from S2 and Figure 18 represents the resulting histogram from S3. The histograms show that the inter-class and intra-classes extend over each other. The area of overlap within the S2 segmentation method is less than what is observed in the S1 method, yet it exceeds that of the S3 method. Consequently, in terms of precision, the S3 segmentation outperforms the other segmentations.

Figure 19. Accuracy for all segmentations, N=20

Figure 19 shows the accuracy of the system under different scenarios (S1 E1, S1 E2, S1 E3, S2 E3, S3 E1, S3 E2, S3 E3) and different noise levels (from 0 to 0.005). The accuracy of the system generally decreases as the noise level increases, in all scenarios. This means the system becomes less accurate as the environment becomes noisier, which is a common trend in many systems. At a glance, it seems that the scenarios S3 E1, S3 E2, and S3 E3 consistently perform better (have higher accuracy) compared to other scenarios across all noise levels. The S1 E1, S1 E3, and S2 E3 scenarios seem to have the lowest accuracy across all noise levels. The

scenarios S3 E1, S3 E2, and S3 E3 seem to be more robust to noise compared to other scenarios. They maintain relatively high accuracy even as the noise level increases. S1 E1, S1 E3, and S2 E3 show fairly consistent accuracy scores across different noise levels. Despite the presence of noise, the accuracy doesn't seem to decrease significantly.

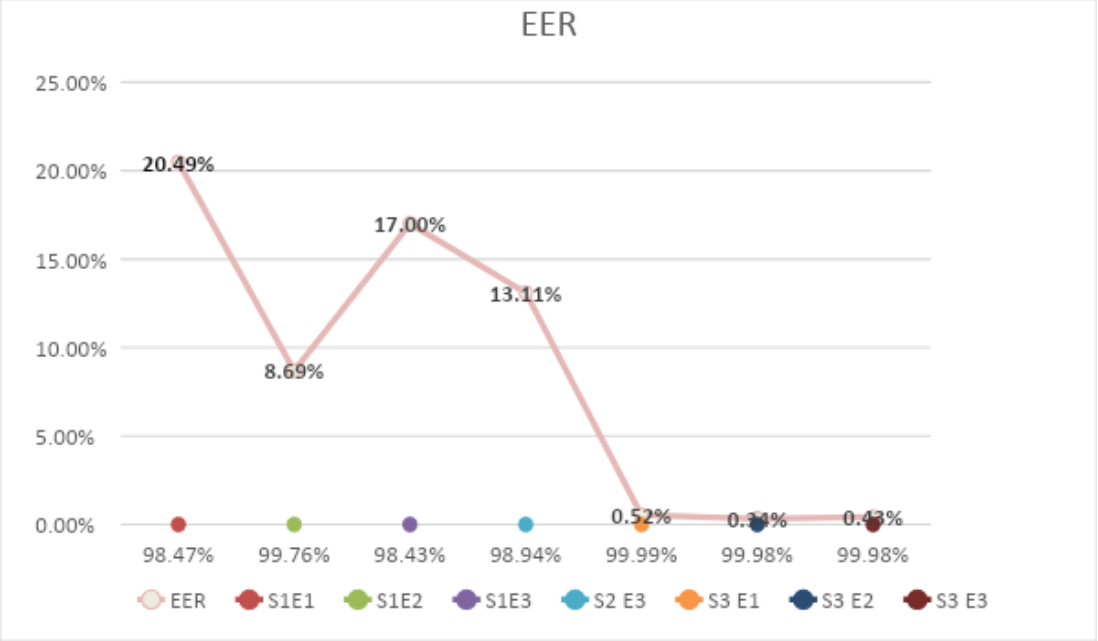

Figure 20. EER and Accuracy for N=20, n=10, noise=0

Figure 20 shows how the Equal Error Rate changes for the same set of individuals using different segmentations and 0 Gaussian noise. By looking at the results it can be said that:

For S1E1, the accuracy is high at 98.47% but the EER is also relatively high at 20.49%. This means that although the model is correctly classifying a high percentage of instances, the rate at which it makes false positive and false negative errors is quite high.

For S1E2, it can be seen an improvement in both accuracy and EER. The accuracy increased to 99.76% and the EER dropped to 8.69%. This suggests that the model performs significantly better under these conditions than it did for S1E1.

S1E3 has a slight drop in accuracy to 98.43% and an increase in EER to 17.00%, suggesting that performance is worse here than in S1E2, but slightly worse than S1E1.

For S2E3, the accuracy improves slightly to 98.94% and the EER decreases to 13.11%. It appears to perform better than all the S1 conditions.

Finally, the S3 combinations (S3E1, S3E2, and S3E3) all have extremely high accuracy, nearly 100%, and extremely low EER (less than 1%), suggesting that the system performs very well under these conditions.

So, based on the results the system appears to perform best under the conditions represented by S3 (S3E1, S3E2, and S3E3), with nearly perfect accuracy and very low error rates. Performance under the S1 and S2 conditions varies but is generally worse, with S1E2 being the best among them.

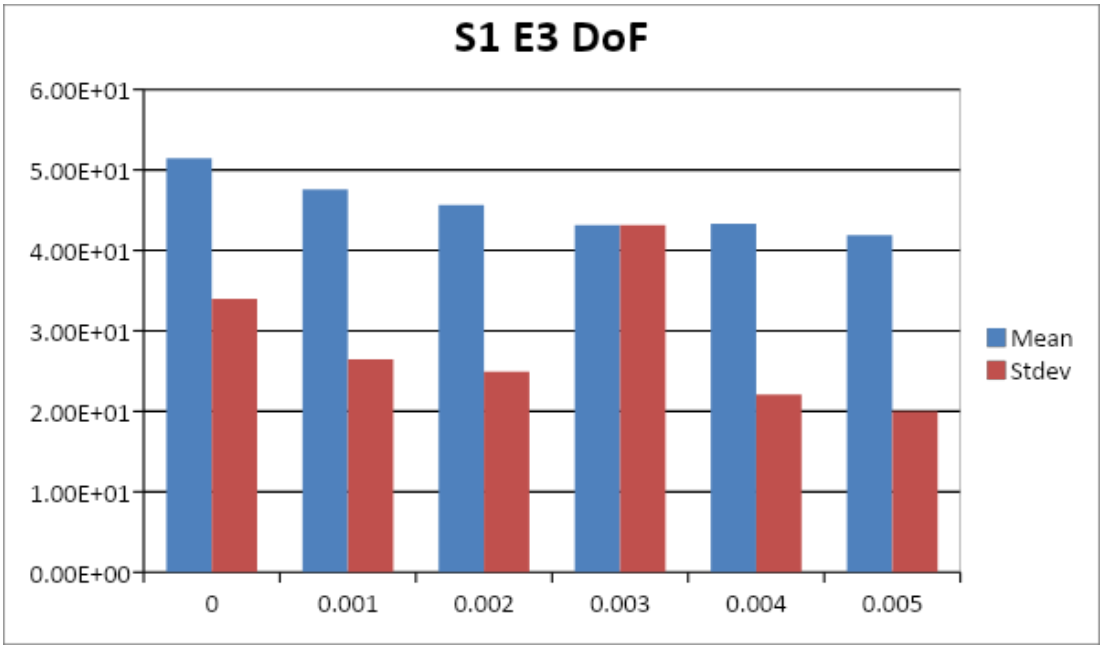

Figure 21. Degree of Freedom for S1 E3, for noise levels 0, 0.001, 0.002, 0.003, 0.004, 0.005

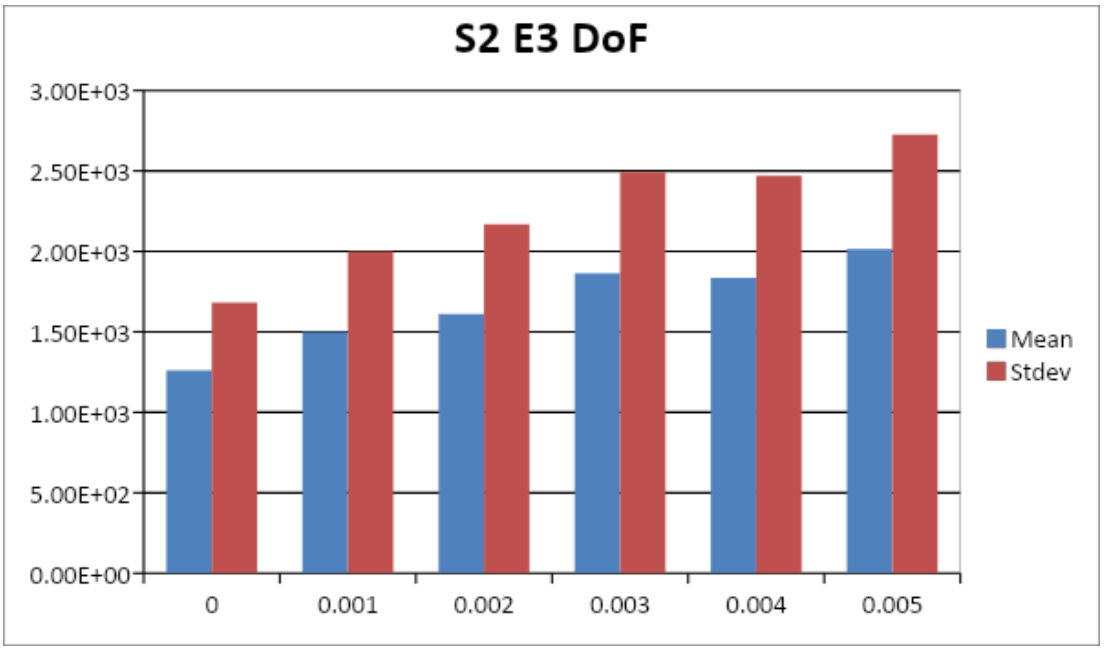

Figure 22. Degree of Freedom for S2 E3, for noise levels 0, 0.001, 0.002, 0.003, 0.004, 0.005

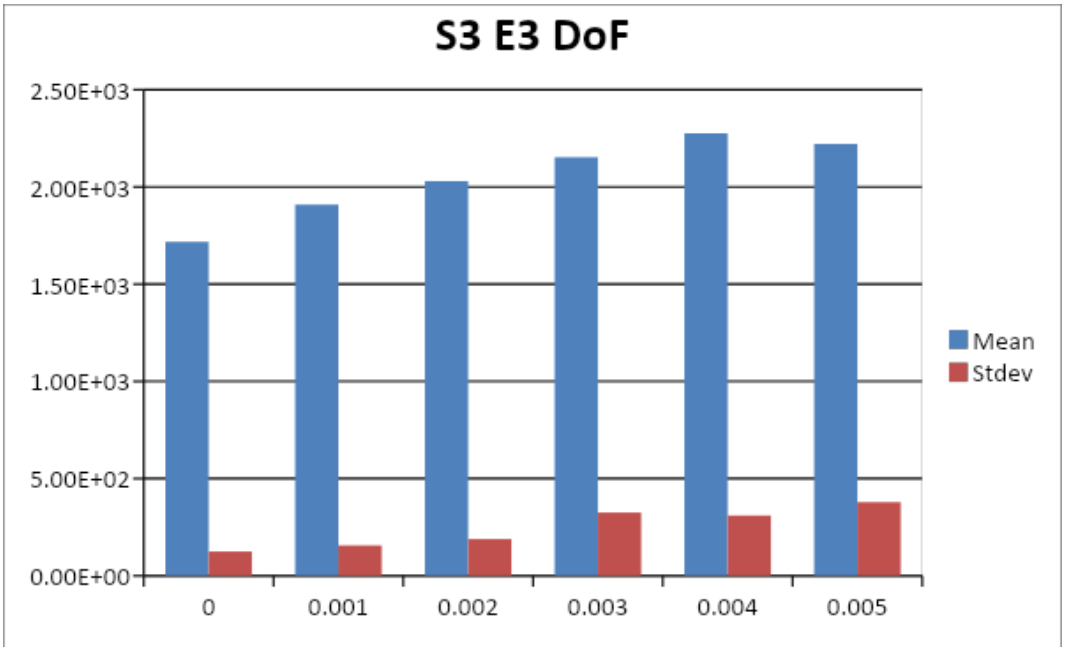

Figure 23. Degree of Freedom for S2 E3, for noise levels 0, 0.001, 0.002, 0.003, 0.004, 0.005

Figure 21, Figure 22 and Figure 23 show how the Degree of Freedom changes for different levels of Gaussian noise. For S1E3, as noise increases, the mean value generally decreases, going from 51.4 at 0 noise to 41.9 at 0.005 noise. This suggests that increasing the noise level decreases the mean value for S1E3. The

standard deviation also generally decreases, suggesting less inconsistency in measurements as the noise increases.

For S2E3, both the mean and standard deviation generally increase as noise levels increase, indicating that both the average value and the inconsistency in measurements increases with increasing noise.

For S3E3, similar to S2E3, both the mean and standard deviation generally increase as noise levels increase. The mean increases from 1720 at 0 noise to 2220 at 0.005 noise, and standard deviation increases from 125 at 0 noise to 378 at 0.005 noise.

These results suggest that noise influences the measurements differently depending on whether you're looking at S1E3, S2E3, or S3E3. This could suggest that S1E3 is more robust to noise, while S2E3 and S3E3 are more sensitive.

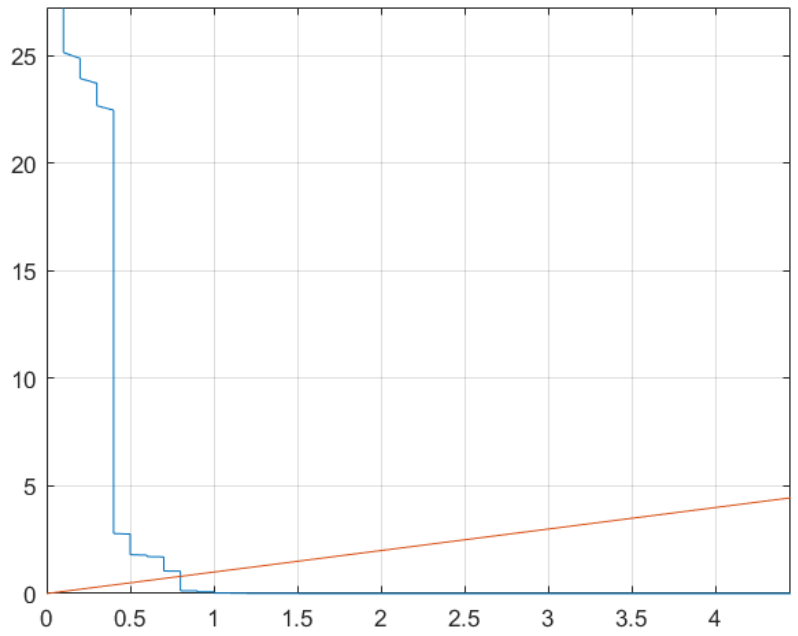

Figure 24. EER of 0.9543for S3, N= 50, n=10

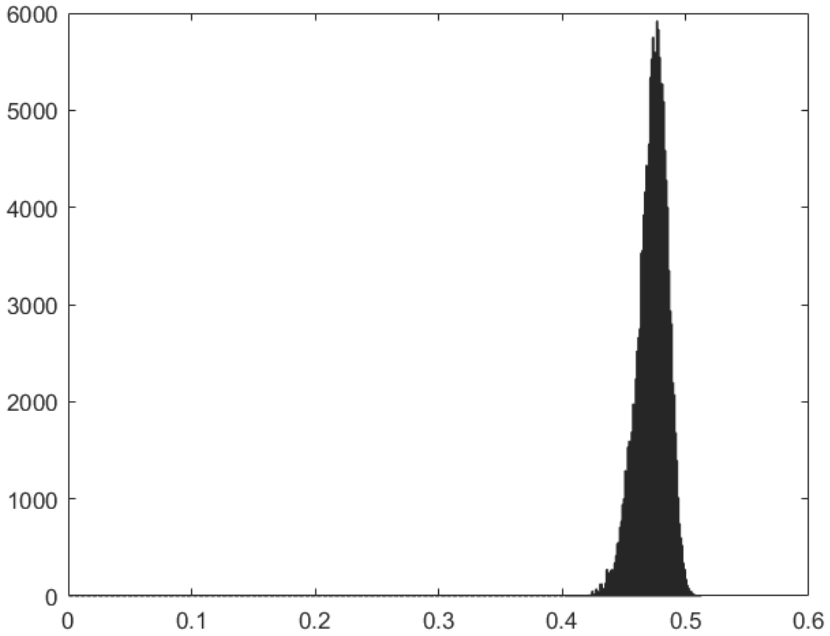

Figure 25. Histogram for N=50, n=10 for S3 segmentation

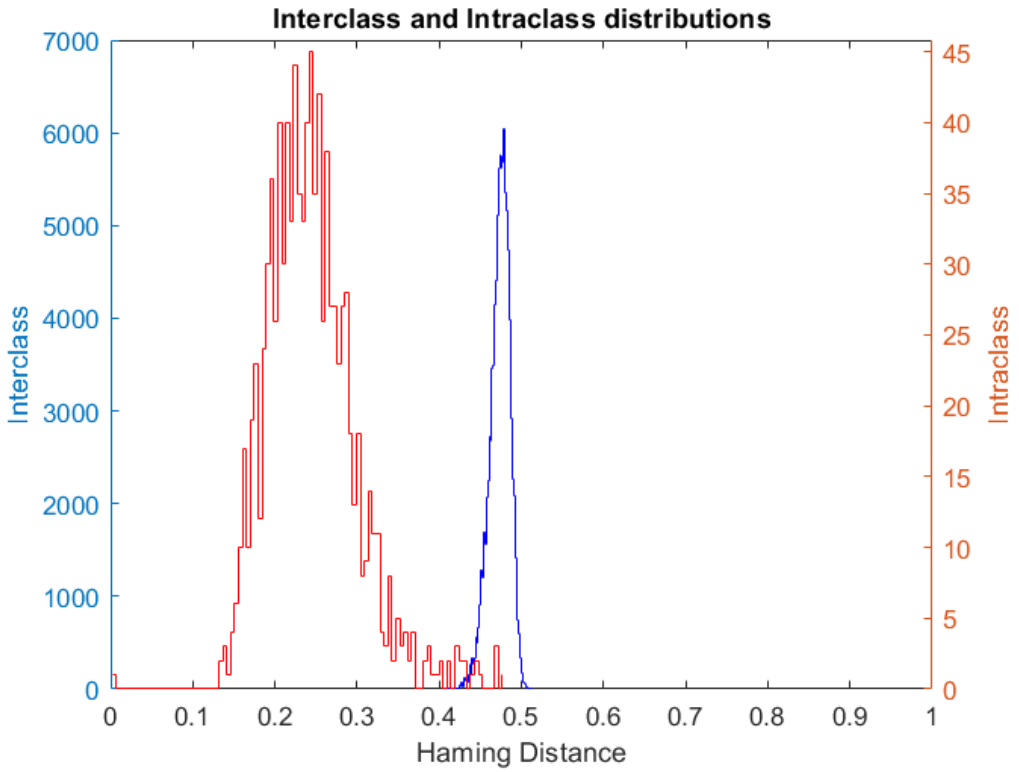

Figure 26. Inter-class and Intra-class distributions for N=50, n=10 for S3 segmentation

Figure 24, Figure 25 and Figure 26 show graphs related to a group of 50 people and 10 images per person using S3. All the graphs prove the points mentioned

previously on the paper regarding S3. Figure 24 shows an EER of 0.9543%. An EER of 0.9543% means that the iris recognition system will, on average, falsely accept unauthorized individuals and falsely reject authorized individuals approximately 0.9543% of the time. In some contexts, a less than 1% error rate might be considered quite good. For example, if this system was being used for a generic access control in a relatively low-security environment, this error rate could be acceptable. However, in high-security environments, such as airports, nuclear facilities, military installations, etc., even a 1% error rate could be considered too high because the consequences of a false acceptance could be severe.

Figure 25 is the respective histogram of S3 segmentation for 50 people using 10 images per person.

Figure 25 show the Inter-class and Intra class distributions for N = 50 and n = 10. Even though an overlap can be distinguished between the two distributions, S3 still performs better than the other segmentations.

CHAPTER 5

CONCLUSIONS

5.1 Conclusions

To summarize, the S3 E1, S3 E2, and S3 E3 combinations show superior performance in terms of accuracy and EER, maintaining high performance even under increasing noise levels. However, their higher DoF values suggest more complex system settings, and while they show good dprime, this ability does decrease as noise increases. Higher degrees of freedom reported in these

combinations may have played a role in their better performance by letting them accommodate more complicated patterns.

On the other hand, the S1 E1, S1 E3, and S2 E3 combinations, while still delivering a quite high level of accuracy, show higher EERs, indicating less optimal performance. The dprime of these configurations also decreases under noise.

The selection between these combinations would depend on the specific use case, the acceptable errors, and the expected level of noise in the system's operating environment. The results suggest that if high accuracy and lower EER are essential and a complex system can be appropriate, then configurations like S3 E1, S3 E2, or S3 E3 would be recommended. On the other hand, if the use case allows for a slightly lower level of accuracy and a higher EER, then combinations like S1 E1, S1 E2, S1 E3, or S2 E3 might be considered.

5.2 Recommendations for future research

Considering that noise contributes significantly to the decrease of iris recognition performance, researching improved noise-reduction techniques could be very helpful. It would also be valuable to explore strategies for improving the system's ability to adapt to various types or amounts of noise.

The observed relationship between system performance and complexity, as shown by DoF, implies that future research might look into techniques to maximize this relationship. This might consist of researching approaches that preserve high accuracy and low EER while reducing system complexity.

Because the ability to distinguish among various irises is essential in iris recognition, additional research could focus on creating ways to improve differentiability, especially in high-noise environments. Studying why particular setups show more drop in dprime as you add noise could yield insights on how to solve this problem.

Considering EER is a balance of FAR and FRR, comprehending how different configurations affect this balance may be beneficial. Further research could concentrate on establishing techniques that improve this equilibrium, resulting in more reliable and effective systems.

Lastly, performing additional studies in a wider range of real-world situations helps reinforce these conclusions and improve overall adaptation. This might imply testing these systems using various iris datasets, in different environments, or with different hardware specifications.

REFERENCES

[1] Hu, X., V.P. Pauca, and R. Plemmons. Iterative directional ray-based iris segmentation for challenging periocular images. in Chinese Conference on Biometric Recognition. 2011. Springer

[2] Gupta, R. and A. Kumar, An Effective Segmentation Technique for Noisy Iris Images. International Journal of Application or Innovation in Engineering & Management, 2013. 2(12): p. 118-125.

[3] X. Liu, K.W. Bowyer, and P.J. Flynn, "Experiments with an improved iris segmentation algorithm," Fourth IEEE Workshop on Automatic Identification Advanced Technologies (AutoID'05), Buffalo, NY, USA, Oct. 2005, pp. 118-123. DOI: 10.1109/AUTOID.2005.21

[4] A. Uka, A. Roçi, and O. Koç, "Improved segmentation algorithm and further optimization for iris recognition," IEEE EUROCON 2017 - 17th Int. Con. on Smart Technologies, Ohrid, 2017, pp. 85-88. DOI: 10.1109/EUROCON.2017.8011082

[5] L. Masek, "Recognition of human iris patterns for biometric identification," BEng Thesis, The Univ. of Western Australia, 2003. https://www.peterkovesi.com/studentprojects/libor/LiborMasekThesis .pdf [accessed: 23 July 2019].

[6] Uka, A., Roçi, A., & Koç, O. (2017, July). Improved segmentation algorithm and further optimization for iris recognition. In *IEEE EUROCON 2017-17th International Conference on Smart Technologies* (pp. 85-88). IEEE.

[7] Koç, O., Tosku, L., Hoxha, J., Topal, A. O., Ali, M., & Uka, A. (2019, August). Detailed Analysis of IRIS Recognition Performance. In *2019 International Conference on Computing, Electronics & Communications Engineering (iCCECE)* (pp. 253-258). IEEE.

[8] Koç, O., Roçi, A., & Uka, A. (2019). Performance analysis of iris recognition by using classical and trapezoidal shaped templates with a state-of-art iris segmentation technique. *Int. J. of Advances in Electronics and Comp. Sci.*, *6*(3), 64-67.

[9] Koç, O., Uka, A., Ali, M., Muda, K., Balla, O., & Roçi, A. (2020, August). Iris Recognition Performance Analysis for Noncooperative Conditions. In *2020 International Conference on Computing, Electronics & Communications Engineering (iCCECE)* (pp. 172-175). IEEE.

[10] Koç, O., & Uka, A. (2016). A new encoding of iris images employing eight quantization levels. *Journal of Image and Graphics*, *4*(2), 78-83.

[11] Koc, O., Balla, O., & Uka, A. (2019). Performance of Convolutional Neural Networks in Biometrics for Noisy Iris Images. In *Proc. of the 3rd MULTI-modal Imaging of FOREnsic SciEnce Evidence Tools for Forensic Science 2019*.

[12] Koç, O., & Uka, A. (2015). Iris recognition by 1D Fourier transform. In Proc. International Scientific Conference Computer Science (pp. 315-320)

[13] MUDA, K. (2019). *IRIS RECOGNITION UNDER NOISE CONDITION* (Master Thesis, EPOKA UNIVERSITY).

[14] Kumar, A., & Passi, A. (2010). Comparison and combination of iris matchers for reliable personal authentication. Pattern recognition, 43(3), 1016-1026.

[15] KLLOGJRI, S. (2022). *ACCURACY OF IRIS RECOGNITION USING TRAPEZOIDAL TEMPLATES* (Master of science, EPOKA UNIVERSITY).

[16] TOSKU, L. (2019). *PERFORMANCE ANALYSIS OF DIFFERENT SEGMENTATIONS, ENCODING SCHEMES AND 2D LOG GABOR FILTER ON LOW QUALITY IRIS IMAGES* (Master of science, EPOKA UNIVERSITY).

[17] ROÇI, A. (2016). *IRIS RECOGNITION* (Master of science, EPOKA UNIVERSITY).

[18] Daugman, J. (2009). How iris recognition works. In *The essential guide to image processing* (pp. 715-739). Academic Press.

[19] Sarode, N. S., & Patil, A. M. (2014). Review of iris recognition: an evolving biometrics identification technology. *International Journal of Innovative Science and Modern Engineering (IJISME)*, *2*(10), 34-40.

[20] Daugman, J. (2007). New methods in iris recognition. *IEEE Transactions on Systems, Man, and Cybernetics, Part B (Cybernetics)*, *37*(5), 1167-1175.

[21] Proença, H., & Alexandre, L. A. (2006). Iris segmentation methodology for non-cooperative recognition. *IEE Proceedings-Vision, Image and Signal Processing*, *153*(2), 199-205.

[22] Koc, O., Roçi, A., & Uka, A. (2016). Iris recognition and a new approach in encoding. *J. of Natural and Technical Sciences*, *21*(1), 89-101

APPENDIX

Custom code to create histogram of inter and intra class distributions

```
% Histogram calculations
[binsInter, edgesInter] = histcounts(inter, 100);
[binsIntra, edgesIntra] = histcounts(intra, 100);

% Average edges for plotting
xInter = mean([edgesInter(1:end-1); edgesInter(2:end)]);
xIntra = mean([edgesIntra(1:end-1); edgesIntra(2:end)]);

figure(1);
yyaxis left
stairs(xInter, binsInter, 'blue')
ylabel('Interclass')

hold on
yyaxis right
stairs(xIntra, binsIntra, 'red')
ylabel('Intraclass')

xlabel('Haming Distance')
title('Interclass and Intraclass distributions')

% set the x-axis limit
xlim([0 1])

% Save the figure
saveas(gcf,'figure1.png')
```